Enhancements in lower stratospheric CH_3CN observed by the Upper Atmosphere Research Satellite Microwave Limb Sounder following boreal forest fires

Nathaniel J. Livesey,[1] Michael D. Fromm,[2] Joe W. Waters,[1] Gloria L. Manney,[1,3] Michelle L. Santee,[1] and William G. Read[1]

Received 8 August 2003; revised 2 December 2003; accepted 9 December 2003; published 23 March 2004.

[1] On 25 August 1992, the Microwave Limb Sounder (MLS) on the Upper Atmosphere Research Satellite observed a significant enhancement in the abundance of lower stratospheric methyl cyanide (CH_3CN) at 100–68 hPa (~16–19 km altitude) in a small region off the east coast of Florida. The enhancement was seen to decay and move generally westward over ~6 days. Concentrations up to ~1500 parts per trillion by volume (pptv) were observed, compared to a typical stratospheric background level of 30 pptv. Aerosol index data from the Nimbus 7 Total Ozone Mapping Spectrometer (TOMS) instrument, together with trajectory calculations, provide strong evidence that the enhancement arose from the stratospheric injection, associated with strong thunderstorms, of tropospheric air with high CH_3CN concentrations, originating in regions of extensive forest fire activity in Idaho (not observed by MLS in this period because of orbital geometry). After being lofted into the lower stratosphere, this air was advected into the regions observed by MLS and subsequently dispersed. These MLS enhanced CH_3CN observations add to the growing body of evidence for the occurrence of such episodic injections of tropospheric air into the stratosphere. *INDEX TERMS:* 0322 Atmospheric Composition and Structure: Constituent sources and sinks; 0368 Atmospheric Composition and Structure: Troposphere—constituent transport and chemistry; 3314 Meteorology and Atmospheric Dynamics: Convective processes; *KEYWORDS:* methyl cyanide, biomass burning, convective events

Citation: Livesey, N. J., M. D. Fromm, J. W. Waters, G. L. Manney, M. L. Santee, and W. G. Read (2004), Enhancements in lower stratospheric CH_3CN observed by the Upper Atmosphere Research Satellite Microwave Limb Sounder following boreal forest fires, *J. Geophys. Res.*, *109*, D06308, doi:10.1029/2003JD004055.

1. Introduction

[2] Methyl cyanide (CH_3CN, also known as acetonitrile) is a comparatively long-lived minor constituent in the Earth's atmosphere. Its main source in the troposphere is biomass burning [*Arijs and Brasseur*, 1986; *Hamm and Warneck*, 1990; *de Gouw et al.*, 2003]. Observations of tropospheric CH_3CN [*Snider and Dawson*, 1984; *Singh et al.*, 2003] have indicated typical abundances of 50–200 parts per trillion by volume (pptv), although earlier observations indicated much higher abundances of 7000 pptv [*Becker and Ionescu*, 1982]. However, in regions of forest fire activity, enhancements in tropospheric CH_3CN as high as $\sim 10^6$ pptv have been observed [*Holzinger et al.*, 1999].

[3] The behavior of CH_3CN in the stratosphere is not completely understood. Its primary loss mechanism is reaction with the OH radical, the lifetime with respect to which has been estimated to be ~20 years at 20 km [*Arijs and Brasseur*, 1986]. The Upper Atmosphere Research Satellite (UARS) Microwave Limb Sounder (MLS) instrument provided the first global measurements of stratospheric CH_3CN [*Livesey et al.*, 2001]. These show a persistent peak in CH_3CN abundance in the tropical stratosphere between ~30 and 10 hPa (25–30 km), which is thought to be evidence for an in-situ chemical source [*Livesey et al.*, 2001]. As yet, no independent observations of tropical stratospheric CH_3CN have been made to corroborate this observation.

[4] The MLS instrument [*Barath et al.*, 1993] is one of ten instruments on the UARS platform, which was launched in September 1991. MLS observes thermal microwave emission from the Earth's limb in three spectral regions. The CH_3CN data from MLS are based on observations of emission from a cluster of rotational lines around 202.3 GHz. The CH_3CN spectral signature observed by MLS typically has an amplitude of ~0.2–0.5 K brightness temperature through most of the stratosphere, corresponding to abundances of ~10–50 pptv. The data discussed here are taken from 'version 5' of the UARS MLS data set [*Livesey et al.*, 2003].

[5] MLS observes the atmosphere from one side of the spacecraft, which is in a 56° inclined orbit whose plane precesses by 7° per day. This means that MLS observes the

[1]Jet Propulsion Laboratory, California Institute of Technology, Pasadena, California, USA.
[2]Computational Physics, Inc., Springfield, Virginia, USA.
[3]Also at New Mexico Highlands University, Las Vegas, New Mexico, USA.

0148-0227/04/2003JD004055$09.00

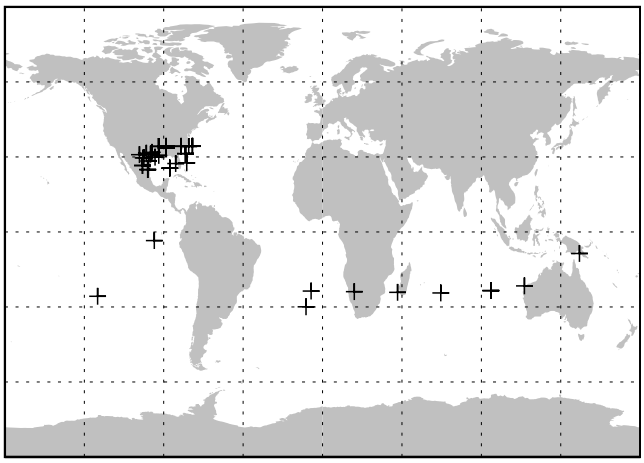

Figure 1. "Spikes" in Microwave Limb Sounder (MLS) CH_3CN over the period 14 August to 20 September 1992, identified by routine analysis. The plus symbols represent the locations of all >4σ spikes that the data processing algorithms have identified as "good quality" data (i.e., good radiances and good fits to those radiances).

atmosphere from 80° latitude in one hemisphere to 34° in the other. Every ~36 days, the spacecraft executes a 180° yaw maneuver (in order to keep one side of the spacecraft in continuous darkness). Thus every ~36 days (a 'UARS month'), MLS switches between making the majority of its observations in the northern or the southern hemisphere.

2. Localized Stratospheric CH_3CN Enhancement Seen by the Microwave Limb Sounder (MLS) in Late August 1992

[6] As part of the UARS MLS version 5 data quality assessment exercise, the science team studied the occurrences of 'spikes' in the MLS data each UARS month. These spikes were defined as values outside 4 standard deviations of the ensemble of MLS data within 6° latitude bins over the UARS month. The most dramatic finding of this spike survey was a cluster of spikes seen in CH_3CN over the south-eastern United States and Gulf of Mexico during the August/September 1992 UARS month. These are shown in Figure 1 and are the subject of this paper.

[7] Closer analysis of the data showed that there was a dramatic enhancement in lower stratospheric (100–68 hPa) CH_3CN in a tightly confined region, first seen on 25 August 1992. The region of enhancement moved generally westward and dispersed over a period of a few days. Figure 2 shows MLS CH_3CN observations at 100 and 68 hPa over a six day period, starting on 25 August 1992. Nothing unusual is seen in the CH_3CN data before this date, or at pressures smaller than 68 hPa on any date in this period (MLS does not measure CH_3CN abundances at pressures >100 hPa).

[8] It is essential to bear in mind that during this time MLS was making no observations north of 34°N (as evident in Figure 2). This is a consequence of the UARS 'yaw cycle' described in section 1. Thus it is impossible to tell from the MLS data alone whether these observations represent a small localized event or the tip of some much larger enhancement northward of the MLS observing range.

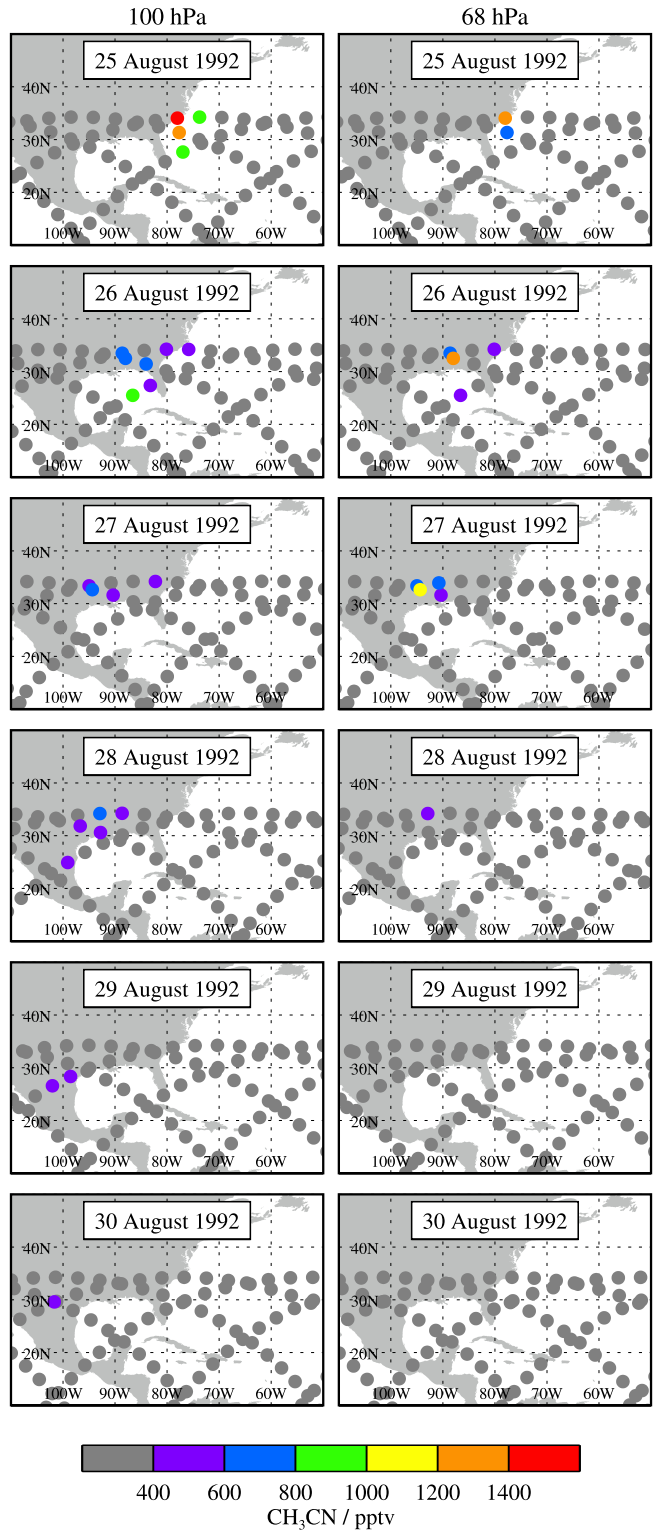

Figure 2. Individual MLS CH_3CN observations at 100 hPa (left) and 68 hPa (right) for six days in August 1992. Typical values at these altitudes are 10–30 pptv.

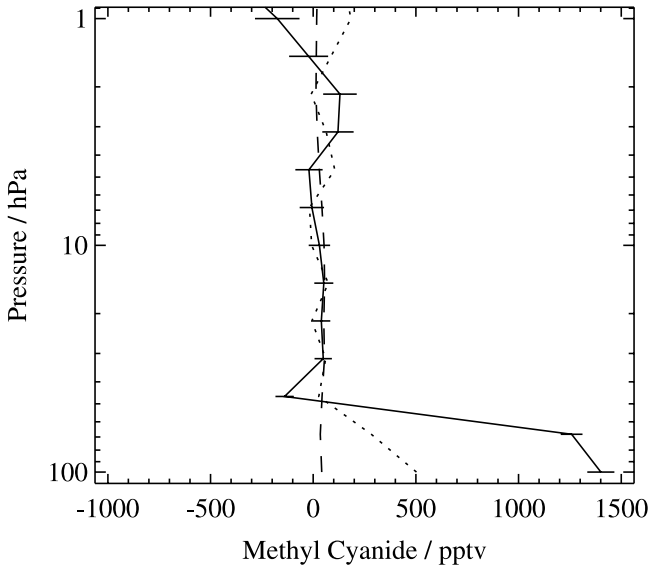

Figure 3. Sample MLS CH_3CN profile data during the enhancement event. The solid line shows the profile for 25 August 1992, corresponding to the 100 hPa red data point (profile 424) shown in Figure 2. The error bars on this line indicate the precision uncertainty on this profile due to radiance noise. The dotted line shows the profile corresponding to the purple 100 hPa point (profile 533) on 30 August 1992 (error bars are omitted here for clarity, but are little different from those for the solid line). The dashed line shows typical profiles for July at the equator (taken from Figure 2 of [*Livesey et al.*, 2001]).

[9] Figure 1 also shows a band of spikes around 25°S. These are all observations taken on 19 September 1992. A study of the MLS radiance measurements indicates that there is probably enhanced SO_2 in this region (see section 2.2 for a discussion of the spectral similarity of CH_3CN and SO_2 in the MLS observations).

2.1. MLS Profile Observations

[10] Figure 3 shows sample MLS CH_3CN profiles during the August 1992 event. The enhancements are seen to be significant compared to the precision expected on the MLS CH_3CN observations from radiance noise considerations. In general, the MLS 100 hPa CH_3CN observations are considered unreliable because of overlapping spectral signatures from other molecules (e.g., $H_2{}^{18}O$), which have less impact at smaller pressures [*Livesey et al.*, 2001]. In this case, however, the signal is so strong that such ambiguity is insignificant. The accuracy of MLS CH_3CN data is estimated in general to be 10 pptv + 20% [*Livesey et al.*, 2001]. In cases such as this, however, one also has to consider how well MLS observes vertically sharp features in CH_3CN.

[11] The MLS retrieval algorithms use all the radiance observations with limb tangent pressures <150 hPa. The MLS field of view has a Gaussian form, ~6 km wide in the vertical. Limb observations in this altitude region are made at a vertical spacing of around 2.5 km. Although the retrieval algorithms account for all these factors, it is difficult to completely characterize the vertical location and extent of sharp CH_3CN enhancements, and it is possible that the large 100 hPa and 68 hPa values reported could be indicative of CH_3CN enhancements at pressures as great as 150 hPa, which is still in the stratosphere in this region.

2.2. MLS Radiance Observations

[12] Figure 4 shows the limb radiance observations corresponding to the solid profile shown in Figure 3, along with 'typical' observations and observations of volcanically enhanced SO_2, which, as can be seen, is spectrally similar to CH_3CN. It is possible to estimate an upper limit for the SO_2 contribution to these observations by examining the radiance observations in UARS MLS band 4 (not shown). Observations from the Mount Lascar event in this band show a clear ~1.4 K signal, corresponding to ~60 ppbv SO_2. In the August 1992 data, on the other hand, significant

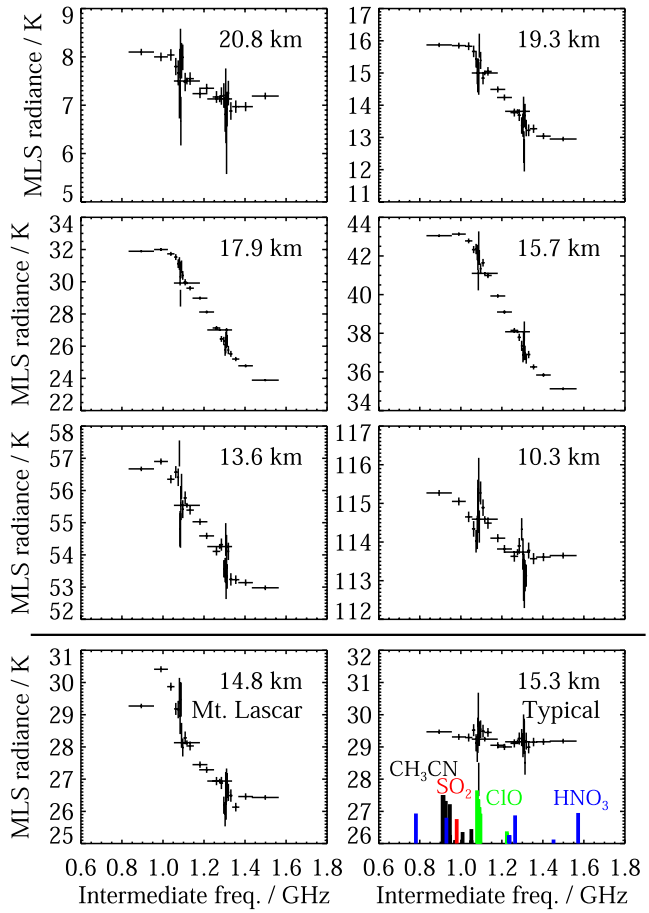

Figure 4. MLS radiance observations in bands 2 and 3. The upper three rows show a selection of the observations corresponding to the solid profile in Figure 3. The lower row shows observations of enhanced SO_2 (~60 ppbv) following the Mount Lascar eruption on 21 April 1993 (left), and tropical observations on 17 September 1992, typical of nonenhanced situations (right). The vertical axes are radiances expressed as equivalent brightness temperatures in Kelvin, with the vertical error bars indicating 1σ levels for radiance noise (the horizontal bars indicate the bandwidth of the MLS channels). The altitude of the limb tangent point is denoted in the upper right of each plot. The colored bars under the "Typical" plot denote the positions and relative strengths of the significant spectral lines in this region.

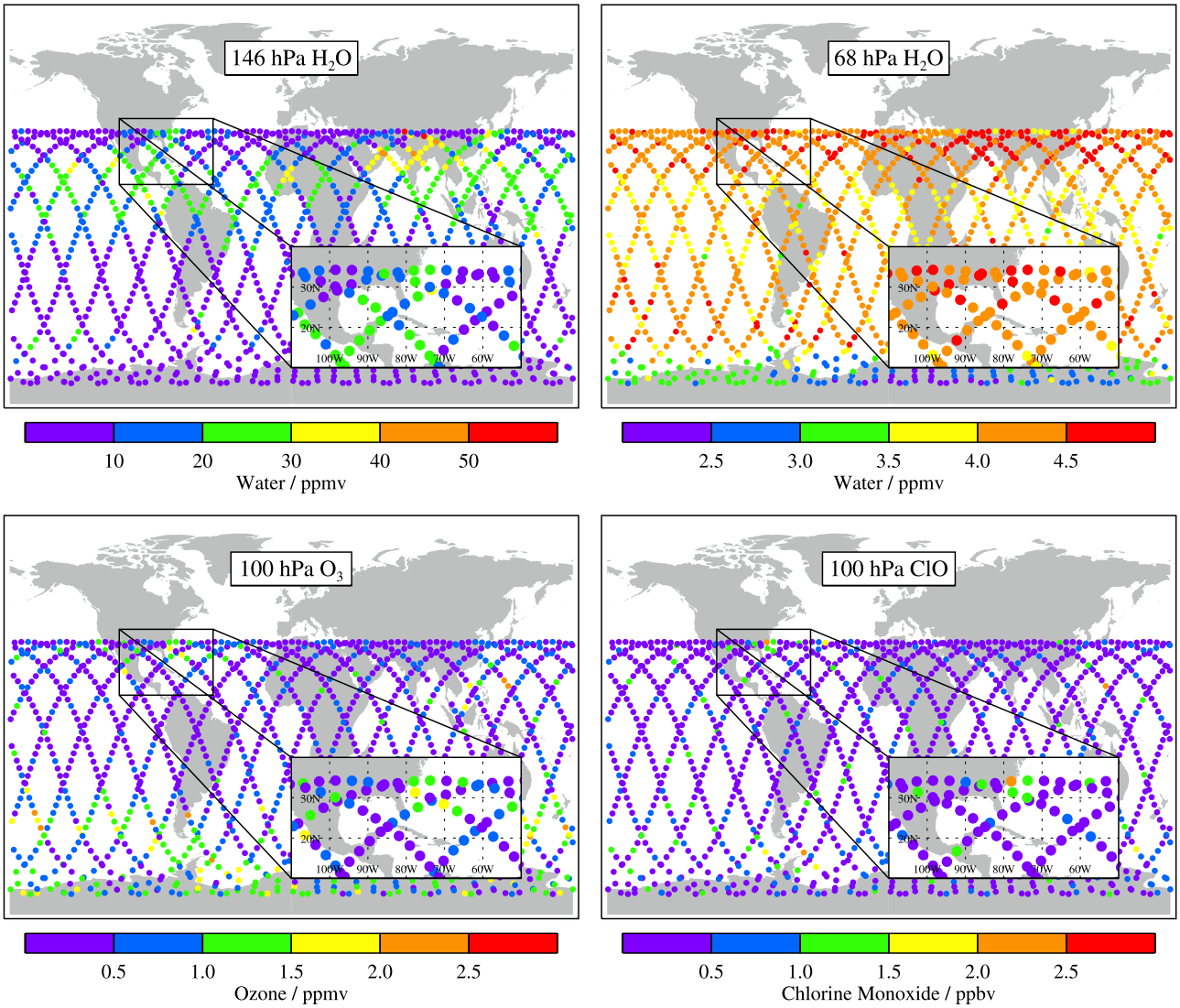

Figure 5. MLS H_2O, O_3 and ClO observations on 25 August 1992. The ozone shown is taken from the 205-GHz radiometer data. The MLS version 5 data set does not include useful observations of water vapor at 100 hPa. The precision of the data points shown is comparable to one color interval in each case.

emission from SO_2 in band 4 is hard to discern. We estimate an upper limit to its possible magnitude of 0.5 K, which would correspond to ~20 ppbv SO_2. A scaling argument implies that such abundances would lead to spectral features of only ~1.3 K amplitude in bands 2 and 3. As the features observed are ~8 K, we conclude that the emission here is dominated by CH_3CN, not SO_2.

[13] We will later show that the most likely origin of this event is pollution from a boreal forest fire. Studies indicate a 1.0 to 0.19 mass emission ratio for SO_2 to CH_3CN is expected from such fires [*Andreae and Merlet*, 2001, and references therein]. Our observations of ~1.4 ppbv enhanced CH_3CN would thus imply abundances of ~5 ppbv SO_2 are to be expected, assuming the CH_3CN and SO_2 life times are comparable.

2.3. Other MLS Observations in the Enhancement Region

[14] The CH_3CN enhancement does not seem to be accompanied by any dramatic enhancement in other species observed by MLS. Figure 5 shows MLS observations of ozone and water in the upper troposphere/lower stratosphere on 25 August 1992. The features seen in these species are within the variability typically seen in their retrieved values from MLS, so, at least from a statistical standpoint, it is hard to relate them to the CH_3CN enhancement.

[15] The figure also shows MLS observations of lower stratospheric ClO which, as seen in Figure 4, are taken from the same spectral region as CH_3CN. The spectral signatures of ClO and CH_3CN in the MLS radiances are not completely orthogonal. Therefore in cases such as this where unusually large CH_3CN signals are present, one might expect some atypical biases in the MLS ClO data. The larger than normal ClO abundances reported by MLS in the CH_3CN enhancement region are probably not, therefore, representative of any real enhancement of ClO in the lower stratosphere.

[16] Unfortunately, no aerosol profile data are available from the Cryogenic Limb Array Etalon Spectrometer (CLAES) instrument, also on UARS, in the enhancement

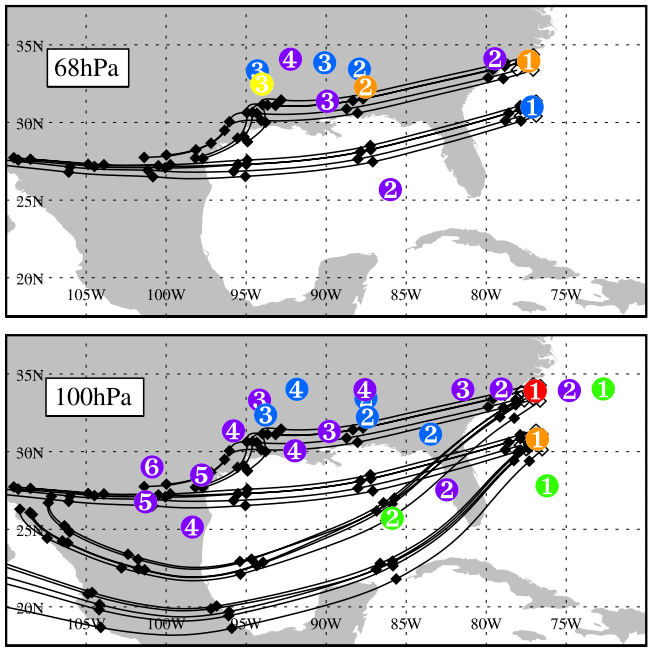

Figure 6. A comparison of the observed behavior of the CH_3CN enhancement with the results of trajectory calculations at 68 and 100 hPa. Trajectories have been run forward from the locations indicated by the (somewhat obscured) hollow diamonds, clustered around the CH_3CN observations on 25 August 1992. The solid diamonds indicate the locations of trajectory points at noon UT on each successive day, with the first set (very close to the start of the trajectories) indicating noon on 25 August 1992. The enhanced MLS data are shown with colored labels; the color indicates the CH_3CN mixing ratio, as in Figure 2, while the numbers in the symbols indicate the day of observation, where day "1" is 25 August 1992. The points corresponding to observations of nonenhanced CH_3CN (shaded in Figure 2) are omitted for clarity.

region. Some profiles are missing because of instrument calibration activities; others were not produced as the retrieval calculations failed to converge (J. Mergenthaler, personal communication, 2000).

2.4. Description of Trajectory Calculations

[17] Trajectory calculations provide a powerful tool for the investigation of this event. All the trajectory computations used here are as described by [*Manney et al.*, 1994]. The calculations use UK Met Office winds and temperatures, with a radiation code to estimate diabatic descent rates. For levels below 375 K potential temperature, an isentropic version of the code was used, since the algorithm that models diabatic motions is not valid in this region. The trajectories in this study are launched from the geographic location of the limb tangent point when MLS was observing the appropriate altitude, as opposed to launching them from the reported location of the MLS profiles. The two are displaced by ~140 km because of the ~7 km s^{-1} movement of the spacecraft during the MLS scan.

[18] Figure 6 compares the MLS observations of enhanced CH_3CN on successive days with the results of trajectory calculations initialized at the locations of two of the earliest enhancement observations. At 68 hPa the agreement between the trajectories and the MLS observations is quite good. Trajectories launched from other enhanced locations (not shown) present a consistent picture.

[19] The trajectories launched at 100 hPa, however, do not represent good agreement with the MLS observations. Furthermore, other trajectories launched at 100 hPa from later MLS observations (not shown) follow quite different paths, yielding a more confusing picture. The Met Office wind data at 100 hPa during this period indicate relatively weak winds and large day-to-day variability in the circulation in this region compared to other regions and periods. This may be associated with the presence of Hurricane Andrew, which passed over the southern tip of Florida and into the northern Gulf of Mexico over the period from 24–25 August 1992. These factors may impact the accuracy of the trajectory calculations in this area. Again, it is important to note that there were no MLS observations north of 34°N. It therefore is possible that some of the later enhancements seen, such as the profile at 34°N, 92°W on 28 August 1992 (day '4'), represent a fresh influx of CH_3CN-enhanced air into the regions observed by MLS, rather than the transport of the enhancements seen on 25 August.

[20] Trajectory calculations can also be used to trace the origin of the air in the CH_3CN enhancement region. Figure 7 shows a set of backward trajectories, along with locations of other events whose significance is discussed in later sections.

[21] The next two sections detail the various hypotheses for the origin of the lower stratospheric CH_3CN enhancement. First we describe two early hypotheses, now thought unlikely to be the cause. Then we present the hypothesis we consider the most likely explanation for the event.

3. Early Hypotheses for the CH_3CN Enhancement

3.1. Failed Launch of Atlas/Centaur-71, 22 August 1992

[22] On 22 August 1992 at 22:40 UT, the launch from Cape Kennedy of an Atlas I rocket carrying a Centaur upper

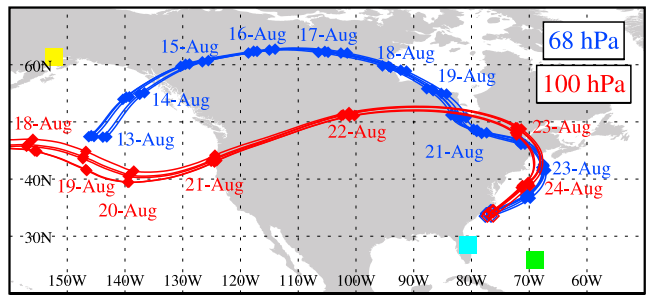

Figure 7. A set of backward trajectories launched at 68 hPa (blue) and 100 hPa (red) on 25 August 1992 from the locations of selected MLS observations of enhanced CH_3CN. The diamond symbols have the same meaning as in Figure 6. Trajectories launched at pressures around 150 hPa (not shown) look similar to those from 100 hPa. The colored boxes indicate the locations of Kennedy Space Center (cyan), the destruction of Atlas/Centaur-71 (green), and Mount Spurr Alaska (yellow).

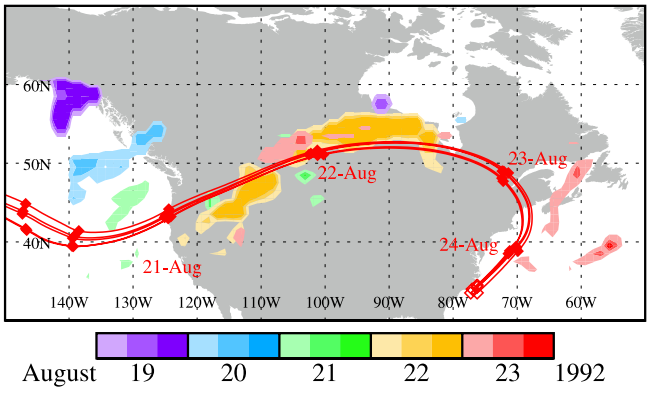

Figure 8. Total Ozone Mapping Spectrometer (TOMS) aerosol index for days preceding the MLS CH_3CN enhancement. The different days are represented by different sets of three colored contours, each with values at 1.5, 2.5, and 3.5. Note the large enhancement on 22 August (this does not obscure significant values on earlier days in this figure). For clarity, the 100 hPa trajectory shown in red in Figure 7 has been repeated here.

stage and a Galaxy 1-R satellite was aborted when the second stage failed to ignite. The self destruct sequence was initiated 8 min after launch, when the spacecraft was at 161 km altitude (S. Scruggs, Patrick Air Force Base, personal communication, 1999). Our first hypothesis was that the observed enhancement in CH_3CN was somehow linked to this event. It is thought that significant portions of the payload (satellite, booster stage, etc.) could have survived the descent through the upper atmosphere (S. Kent, Hughes Space Technology, personal communication, 2000), with their temperature reaching a peak at around 20 km altitude. CH_3CN has been identified as a possible combustion product of hydrazine (fuel for the satellite attitude control system) and of the many polymer components of the satellite.

[23] There are, however, several deficiencies in this hypothesis. Figure 7 shows that the backward trajectories from the enhancement region do not pass close to the location of the self destruct initiation. While the payload descent was probably not completely vertical, horizontal motion of the magnitude required to bring it closer to the trajectories is unlikely. The timing is also suspect, with the destruction event occurring ~56 hours before the first MLS observations of enhanced CH_3CN, (though the enhanced region could have been more confined on earlier days, and fallen in the gaps between the MLS observations.) Finally, this hypothesis cannot easily account for the observed CH_3CN mass loading. We estimate a lower limit on the total mass of enhanced CH_3CN by assuming that it is initially confined to the region directly observed by MLS during the first limb scan that showed enhancement. This region is ~300 km along the limb line of sight and 10 km across it, and the enhanced CH_3CN has a ~50 hPa extent in pressure. The observed mixing ratios of ~1000 pptv thus give a lower limit on the mass of ~2000 kg. By its nature, this will be an extremely conservative lower limit, as all the evidence is that, by the time it is observed by MLS, the enhancement has a significantly larger horizontal extent. This mass is inconsistent with the ~1300 kg mass of the satellite. Unless unusual chemistry associated with the high temperatures of the disintegrating spacecraft is postulated, it is not possible to ascribe the observed CH_3CN enhancement to the destruction of the rocket.

3.2. The Eruption of Mount Spurr in Alaska

[24] Our second hypothesis was that the CH_3CN enhancement observed by MLS was in some way due to the eruption of Mount Spurr in Alaska on 18 August 1992. This hypothesis arose from the study of TOMS aerosol observations [*Krotov et al.*, 1997; *Torres et al.*, 1998] taken on the days before the CH_3CN enhancement event, shown in Figure 8. The enhanced aerosol seen on 19, 20, and 21 August over Alaska and the North Pacific is thought to be due to the eruption of Mount Spurr (P. K. Bhartia, personal communication, 2000) (the large region of enhanced aerosol over the central and northern United States on 22 August 1992 is not, however, thought to originate from Mount Spurr; its significance is discussed in the next section.) While the trajectories shown in Figure 7 do not pass close to Mount Spurr, these are only a subset of the many trajectories we have computed, launched from the location of each MLS enhanced CH_3CN profile over a range of heights. A small number of these pass closer to the location of Mount Spurr than those in Figure 7.

[25] This hypothesis has major drawbacks, however, as there is neither evidence nor any theoretical indications that volcanic activity directly leads to enhancements in CH_3CN (G. Brasseur, J. Crisp, personal communications, 2000). While it is possible that the eruption could have led to biomass burning, yielding enhanced CH_3CN, there is no obvious mechanism for this enhanced air to enter the stratosphere in order to be advected to the location of the MLS observations. In addition, the forward trajectory calculations shown in Figure 9 indicate that the Mount Spurr eruption is not likely to be the origin of the observed CH_3CN enhancement. Although the trajectories at 300 hPa clearly favor the hypothesis that much of the aerosol observed in the north Pacific on 19, 20 and 21 August originates from Mount Spurr, none of the trajectories can account for the enhanced 'aerosol' observed over north America on 22 August. While some of the air that was in the lower stratosphere over the volcano at the time of the eruption ends up near the observed CH_3CN enhancement, the bulk of the air ends up further east, where MLS observes

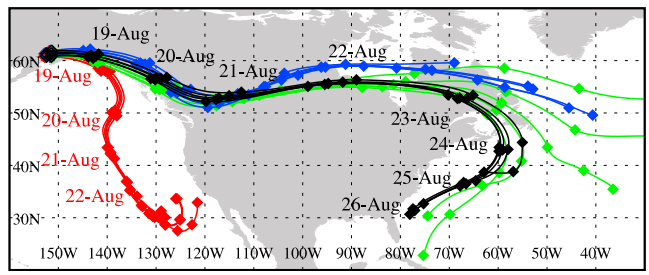

Figure 9. Trajectories launched from the location of Mount Spurr at the time of eruption (18 August, 22:41 UT). Trajectories are launched at 300 hPa (red), 140 hPa (green), 120 hPa (black) and 90 hPa (blue).

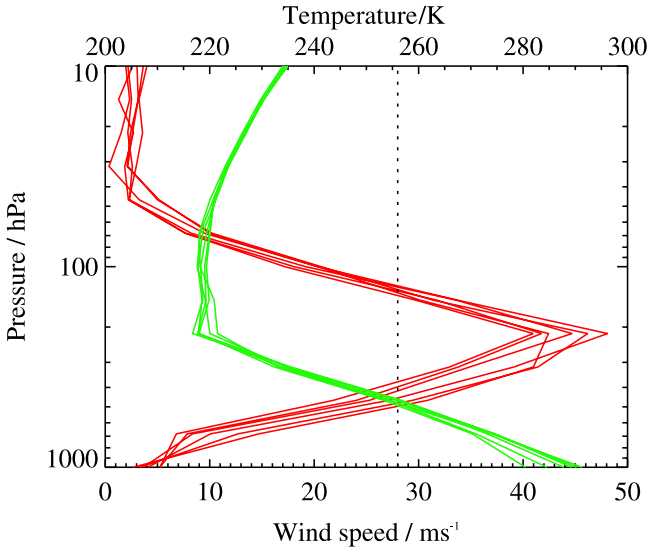

Figure 10. Selected profiles of Met Office wind speed (red, bottom axis) and temperature (green, top axis) within the region of TOMS aerosol index enhancement on 22 August 1992. The dotted line shows the approximate minimum speed of 28 ms^{-1} that would be required to account for the spread of the enhancement region over 24 hours.

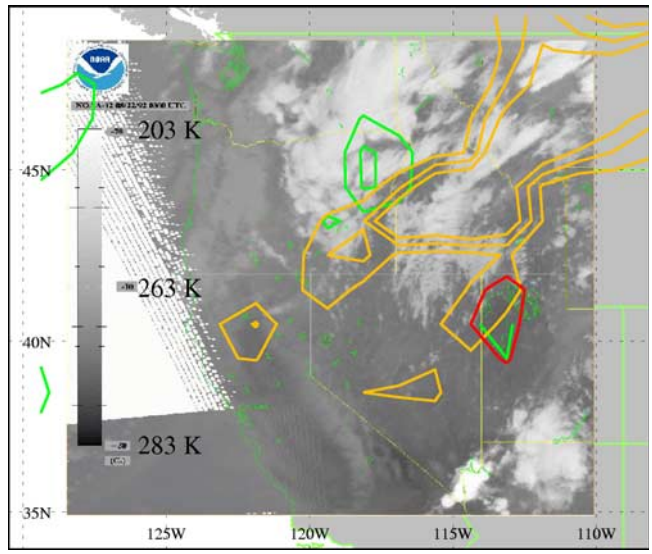

Figure 12. AVHRR infrared image, taken at 03:00 UT on 22 August 1992 for the same region as Figure 11. Storm clouds are seen over NE Oregon, SE Washington and Idaho. Contours are TOMS aerosol index values of 1.5, 2.5, 3.5, as in Figure 8, with green, orange, and red contours again representing 21, 22 and 23 August 1992 respectively.

no unusual enhancements in CH_3CN or any other constituent. Those trajectories from Mount Spurr that do arrive in the enhancement region do so a day later than the first MLS observations of enhanced CH_3CN. From these factors, we conclude that the Mount Spurr eruption is not likely to be the origin of the CH_3CN enhancement observed by MLS.

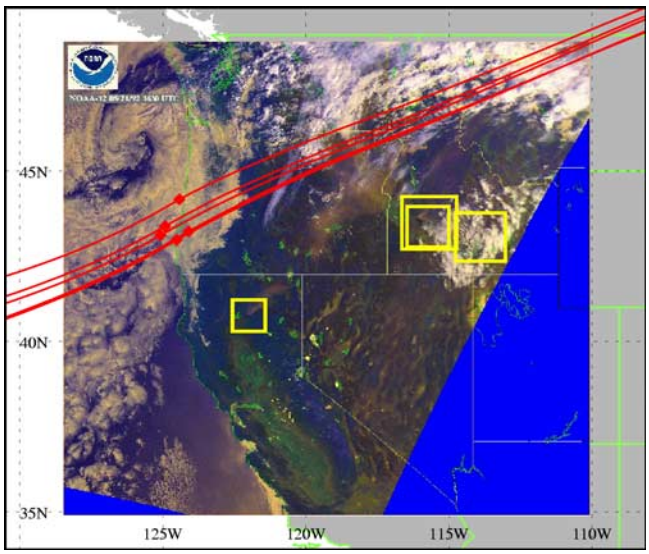

Figure 11. Advanced Very-High Resolution Radiometer (AVHRR) visible image taken at 16:30 UT on 21 August 1992. Smoke is seen over northern California, eastern Oregon and Idaho. The red lines indicate one set of the 100 hPa trajectories from Figure 7, with the diamonds indicating noon UT on the same day. Yellow boxes indicate locations of significant (>20,000 acres) fires in August. For clarity, the area of the box shown is 100 times area of fire.

4. Idaho Forest Fires in August 1992

[26] While the CH_3CN abundances observed are very large for the stratosphere, they are consistent with tropospheric observations in regions of strong pollution (such as biomass burning) [*Becker and Ionescu*, 1982; *Holzinger et al.*, 1999]. This could indicate that the enhancement represents polluted air transported from the troposphere to the stratosphere. However, such transport need not have taken place in the region where the enhancement was first observed.

[27] In the Boise, Idaho region (43°N, 116°W) a large wildfire raged from 19 August to 4 September 1992. This fire burned over 226,000 acres, and was the largest fire since 1910 [Idaho Statesman]. Also, a major complex of thunderstorms occurred in the region around 22 August. Our strongest hypothesis for the origin of the CH_3CN enhancement event is that these storms lofted CH_3CN enhanced tropospheric air into the lower stratosphere. From there the polluted air was advected along the path indicated by our trajectory calculations, into the region observed by MLS ~3 days later. Observation of a tropopause penetration events such as this is not unprecedented. *Fromm et al.* [2000] describe similar events witnessed in Polar Ozone and Aerosol Measurement (POAM) II and Stratospheric Aerosol and Gas Experiment (SAGE) II data. A combination of satellite observations has shown that a similar event occurred in association with a forest fire in Alberta [*Fromm and Servranckx*, 2003].

[28] Figure 8 shows a significant enhancement in TOMS aerosol index on 22 August 1992 that is larger than the 19–21 August enhancement from Mount Spurr. Our hypothesis

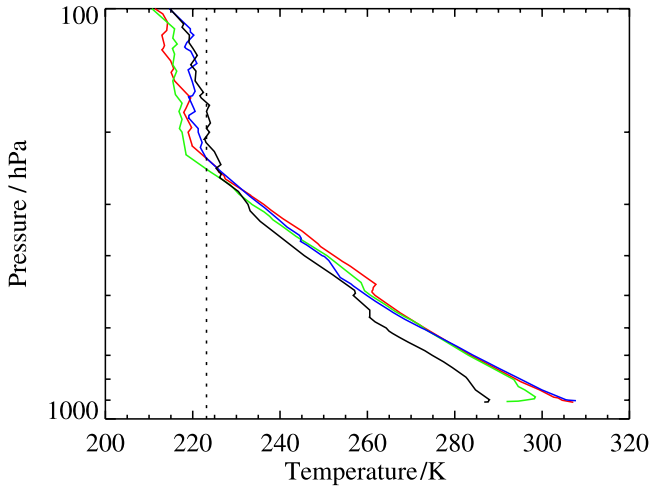

Figure 13. Radiosonde profiles for different times from Boise, Idaho: 21 August 1992 midnight UT (red); 21 August noon (green); 22 August midnight (blue), 22 August noon (black). The dotted line marks the 223 K cloud top temperature from the AVHRR infrared image in Figure 12.

is that this enhancement is smoke and soot in the lower stratosphere originating from the Boise fires. This enhancement is spread over ~2400 km when first observed, with nothing seen in this region the day before. Assuming that the enhancement originates from a more confined region and is spread by the winds, this puts a lower limit of ~28 ms^{-1} on the horizontal wind speed in the region of the aerosol enhancement. Figure 10 shows that such winds are only present in this region between ~500 and ~120 hPa, with the tropopause at ~220 hPa.

[29] Figure 11 shows a visible image from the Advanced Very-High Resolution Radiometer (AVHRR) of the fire region in the morning (local time) of 21 August 1992. Smoke is clearly visible as a brown 'haze' in a band running from around 40°N, 122°W to 45°N, 116°W, near the paths of the estimated trajectories. Figure 12 shows an infrared view of the scene taken roughly 10 hours later, when a breakout of convection was occurring, along with the TOMS aerosol data as shown in Figure 8. The AVHRR infrared data indicate that the cloud top temperature in the center of the enhanced aerosol region is ~223 K, which according to the temperature profiles shown in Figure 13 corresponds to the temperature at or near the tropopause. In regions of strong convective activity, lower tropospheric air is quickly carried to the top of the troposphere. We suggest that in this case penetration of the tropopause occurred, injecting the polluted air into the lower stratosphere.

[30] The TOMS instrument is unable to see aerosol below thick clouds [*Newchurch et al.*, 2001], meaning that this aerosol must be above the cloud tops, and thus in the stratosphere. Taken together with the considerations of the speed of the aerosol spread above, we conclude that much of the aerosol observed by TOMS is located between 220 and 120 hPa. The TOMS aerosol index features between 22 and 23 August generally follow a path of the trajectory, diminish in size, and reside over portions of the Atlantic. Although not shown, that pattern continued through 25 August, when some still-identifiable TOMS aerosol index enhancements were resident close to the CH_3CN enhancements. Thus we contend that the TOMS data offer independent support to our assessment that the MLS enhancements originated with the biomass burning and convection near Boise.

5. Conclusions

[31] The evidence from the independent observations and the trajectory calculations that the enhanced stratospheric CH_3CN observed by MLS has its origins in the Boise forest fire is compelling. This paper provides further strong evidence that extreme convection can quickly carry air from the boundary layer to the lower stratosphere. How frequent such transport events are is hard to ascertain, not least because presumably not all will involve significantly polluted air masses. However, this particular combination of events is clearly somewhat uncommon, as no other lower stratospheric CH_3CN enhancements events of such magnitude are seen in the complete multiyear MLS data set, though a few (~5) shorter lived, more confined enhancements are seen and remain to be fully investigated.

[32] The next generation MLS instrument, to be launched on the EOS Aura spacecraft in 2004, will also be able to measure stratospheric CH_3CN, though the quality of the expected data remains to be fully understood. It is possible that EOS MLS could also produce useful observations of CH_3CN enhancement events in the upper troposphere. However, that possibility has yet to be fully investigated. It will be interesting to see how frequent enhancements of tropospheric CH_3CN are compared to the few lower stratospheric enhancements seen by UARS MLS.

[33] **Acknowledgments.** The authors thank J. Logan, P. K. Bhartia, L. Froidevaux, and A. Krueger for useful discussions. We thank B. P. Ridenoure for research into the events following the August 1992 Atlas-I launch. We thank Brian Stocks of the Canadian Forest Service for providing burn data and George Stephens of NOAA OSEI for the AVHRR imagery. The research in this paper done at the Jet Propulsion Laboratory, California Institute of Technology, was under contract with the National Aeronautics and Space Administration.

References

Andreae, M. O., and P. Merlet (2001), Emission of trace gases and aerosols from biomass burning, *Global Biogeochem. Cycles*, *15*, 955–966.

Arijs, E., and G. Brasseur (1986), Acetonitrile in the stratosphere and implications for positive ion composition, *J. Geophys. Res.*, *91*, 4003–4016.

Barath, F. T., et al. (1993), The upper atmosphere research satellite microwave limb sounder experiment, *J. Geophys. Res.*, *98*, 10,751–10,762.

Becker, K. H., and A. Ionescu (1982), Acetonitrile in the lower troposphere, *Geophys. Res. Lett.*, *9*, 1349–1351.

de Gouw, J. A., C. Warneke, D. D. Parrish, J. S. Holloway, M. Trainer, and F. C. Fehsenfeld (2003), Emission sources and ocean uptake of aceotnitrile (CH_3CN) in the atmosphere, *J. Geophys. Res.*, *108*(D11), 4329, doi:10.1029/2002JD002897.

Fromm, M. D., and R. Servranckx (2003), Transport of forest fire smoke above the tropopause by supercell convection, *Geophys. Res. Lett.*, *30*(10), 1542, doi:10.1029/2002GL016820.

Fromm, M. D., J. Alfred, J. Hoppel, J. Hornstein, R. Bevilacqua, E. Shettle, R. Servranckx, Z. Li, and B. Stocks (2000), Observations of boreal forest fire smoke in the stratosphere by POAM II, SAGE II, and lidar in 1998, *Geophys. Res. Lett.*, *27*, 1407–1410.

Hamm, S., and P. Warneck (1990), The interhemispheric distribution and the budget of acetonitrile in the troposphere, *J. Geophys. Res.*, *95*, 20,593–20,606.

Holzinger, R., C. Warneke, A. Hansel, A. Jordan, W. Lindinger, D. H. Scharffe, G. Schade, and P. J. Crutzen (1999), Biomass burning as a source of formaldehyde, acetaldehyde, methanol, acetone, acetonitrile and hydrogen cyanide, *Geophys. Res. Lett.*, *26*, 1161–1164.

Krotov, N. A., A. J. Krueger, and P. K. Bhartia (1997), Ultraviolet optical model of volcanic clouds for remote sensing of ash and sulfur dioxode, *J. Geophys. Res.*, *102*, 21,891–21,904.

Livesey, N. J., J. W. Waters, R. Khosravi, G. P. Brasseur, G. S. Tyndall, and W. G. Read (2001), Stratospheric CH_3CN from the UARS Microwave Limb Sounder, *Geophys. Res. Lett.*, *28*, 779–782.

Livesey, N. J., W. G. Read, L. Froidevaux, J. Waters, H. Pumphrey, D. Wu, M. Santee, Z. Shippony, and R. Jarnot (2003), The UARS Microwave Limb Sounder version 5 data set: Theory, characterization and validation, *J. Geophys. Res.*, *108*(D13), 4378, doi:10.1029/2002JD002273.

Manney, G. L., R. W. Zurek, A. O'Neill, and R. Swinbank (1994), On the motion of air through the stratospheric polar vortex, *J. Atmos. Sci.*, *51*, 2973–2994.

Newchurch, M., X. Lie, J. Kim, and P. Bhartia (2001), On the accuracy of Total Ozone Mapping Spectrometer retrievals over cloudy regions, *J. Geophys. Res.*, *106*, 32,315–32,326.

Singh, H. B., et al. (2003), In situ measurements of HCN and CH_3CN over the Pacific Ocean: Source, sinks, and budgets, *J. Geophys. Res.*, *108*(D20), 8795, doi:10.1029/2002JD003006.

Snider, J. R., and G. A. Dawson (1984), Surface acetonitrile near Tucson, Arizona, *Geophys. Res. Lett.*, *11*, 241–242.

Torres, O., P. K. Bhartia, J. R. Herman, Z. Ahmad, and J. Gleason (1998), Derivation of aerosol properties from satellite measurements of backscattered ultraviolet radiation: Theoretical basis, *J. Geophys. Res.*, *103*, 17,099–17,110.

N. J. Livesey (corresponding author), G. L. Manney, W. G. Read, M. L. Santee, and J. W. Waters, Jet Propulsion Laboratory, Mail stop 183-701, 4800 Oak Grove Drive, Pasadena, CA 91109, USA. (livesey@mls.jpl.nasa.gov)

M. D. Fromm, Computational Physics, Inc., 2750 Prosperity Ave., Suite 600, Fairfax, VA 22031, USA.